



SINIS bolometer with a suspended absorber

Downloaded from: <https://research.chalmers.se>, 2025-12-05 03:04 UTC

Citation for the original published paper (version of record):

Tarasov, M., Edelman, V., Mahashabde, S. et al (2018). SINIS bolometer with a suspended absorber. Journal of Physics: Conference Series, 969(1). <http://dx.doi.org/10.1088/1742-6596/969/1/012088>

N.B. When citing this work, cite the original published paper.

SINIS bolometer with a suspended absorber

**M. Tarasov^{1,2,3,*}, V. Edelman², S. Mahashabde⁴, M. Fominsky¹, S. Lemzyakov^{2,5},
A. Chekushkin^{1,5}, R. Yusupov^{1,5}, D. Winkler³, and A. Yurgens³**

¹ Kotelnikov Institute of Radio Engineering and Electronics RAS, Mokhovaya 11/7, 125009 Moscow, Russia

² Kapitza Institute for Physical Problems RAS, Kosygina 2, 119334 Moscow, Russia

³ Chalmers University of Technology, Microtechnology and Nanoscience – MC2, Kemivägen 9, Göteborg 41296, Sweden

⁴ Department of Physics-Astrophysics, University of Oxford, Keble Road, OX1 3RH, Oxford, UK

⁵ Moscow Institute of Physics and Technology (State University), Institutsky per. 9, 141700 Dolgoprudny, Russia

*tarasov@chalmers.se

Abstract. We have developed a Superconductor-Insulator-Normal Metal-Insulator-Superconductor (SINIS) bolometer with a suspended normal metal bridge. The suspended bridge acts as a bolometric absorber with reduced heat losses to the substrate. Such bolometers were characterized at 100-350 mK bath temperatures and electrical responsivity of over 10^9 V/W was measured by dc heating the absorber through additional contacts. Suspended bolometers were also integrated in planar twin-slot and log-periodic antennas for operation in the submillimetre-band of radiation. The measured voltage response to radiation at 300 GHz and at 100 mK bath temperature is $3 \cdot 10^8$ V/W and a current response is $1.1 \cdot 10^4$ A/W which corresponds to a quantum efficiency of ~ 15 electrons per photon. An important feature of such suspended bolometers is the thermalization of electrons in the absorber heated by optical radiation, which in turn provides better quantum efficiency. This has been confirmed by comparison of bolometric response to dc and rf heating. We investigate the performance of direct SN traps and NIS traps with a tunnel barrier between the superconductor and normal metal trap. Increasing the volume of superconducting electrode helps to reduce overheating of superconductor. Influence of Andreev reflection and Kapitza resistance, as well as electron-phonon heat conductivity and thermal conductivity of N-wiring are estimated for such SINIS devices.

1. Introduction

Normal Metal-Insulator-Superconductor (NIS) tunnel junctions, as well as SIS junctions, are the main building blocks for superconducting electronics. Single NIS junctions and arrays are used in microwave bolometers, cryogenic thermometers, electron coolers, radiation detectors, etc. In such devices, junctions should fit different parameters for area, transparency, material properties, and thermal characteristics. This leads to various fabrication methods and technique for measurements. Estimations made for equilibrium measurement conditions can be controversial in the case of microwave bolometers, ultra-low temperature thermometers, electron coolers. In Terahertz bolometers, as well as in electron coolers, the energy distribution of electrons can differ from the Fermi-Dirac distribution. In bolometers illuminated with Terahertz radiation, the density of electrons will increase at higher energies, and in



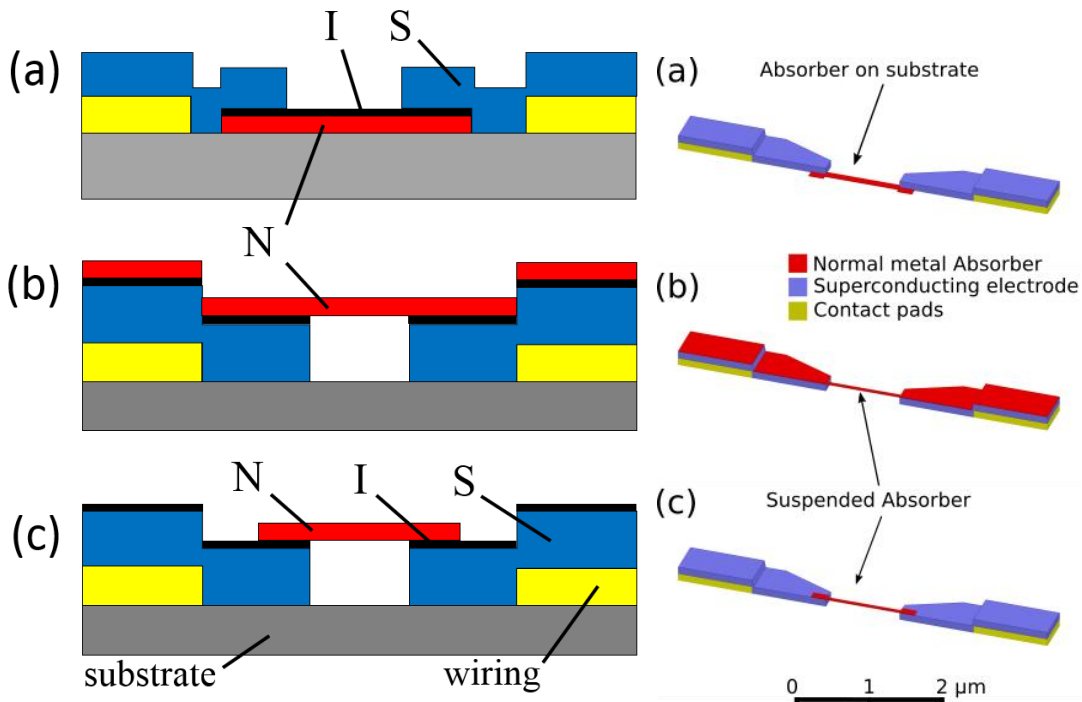


Figure 1. (a) Conventional SINIS bolometer with absorber on the substrate; (b) suspended bolometer with proximity to Au wiring, (c) suspended bolometer with reduced proximity (C). Samples are fabricated on Si substrates with superconducting Al electrodes (blue). The absorber (red) in (a) is oxidized to form a tunnel barrier to superconducting electrode, while in (b), (c) superconducting electrode is oxidized to create a tunnel barrier. Right panel: a 3-d view of the designs.

electron coolers, the distribution will have a reduced density at higher energies. Andreev reflection and proximity effects at the superconductor-normal metal interface induce changes in IV curve compared to simple SIN model and need to be accounted for in the heat-balance equations.

In superconducting bolometers, the electromagnetic radiation raises the temperature T_e of the electron system in a normal-metal absorber. Superconducting leads connected to the absorber through insulating barriers form tunneling junctions. The tunneling current across such a junction is a strong function of T_e , which thereby offers a sensitive readout of the absorbed radiation power. At the low bath temperature T , the absorbed photon energy $hf \gg k_B T$ is distributed among quasiparticles through their multiple interactions and is eventually lost into the cold bath through electrical contacts and through the substrate. Here h is the Planck constant, f is the frequency of incident radiation, k_B is the Boltzmann constant. The balance between the heating radiation and cooling powers determines T_e . Decoupling the absorber from the heat sinks would increase T_e and the detector response through the multiplication of excited electrons. It should be remembered that for the photon energy $hf \gg k_B T_e$, the energy distribution of electrons can be substantially different from the Fermi distribution, depending on the quasiparticle interactions and tunneling rate of the excited electrons through the SIN junction. For estimations of bolometric sensitivity, it is usually assumed that the absorbed radiation is equivalent to a dc Joule heating of the same power.

2. Fabrication

The design of a bolometer with a suspended normal-metal absorber is described below (see Fig.1b and 1c). This fabrication process was inspired by [1]. The fabrication process is simpler compared to the conventional bolometer [2] (Fig. 1a) which uses the shadow evaporation technique. In the design presented here, thin films can be deposited by any physical vapor deposition method including

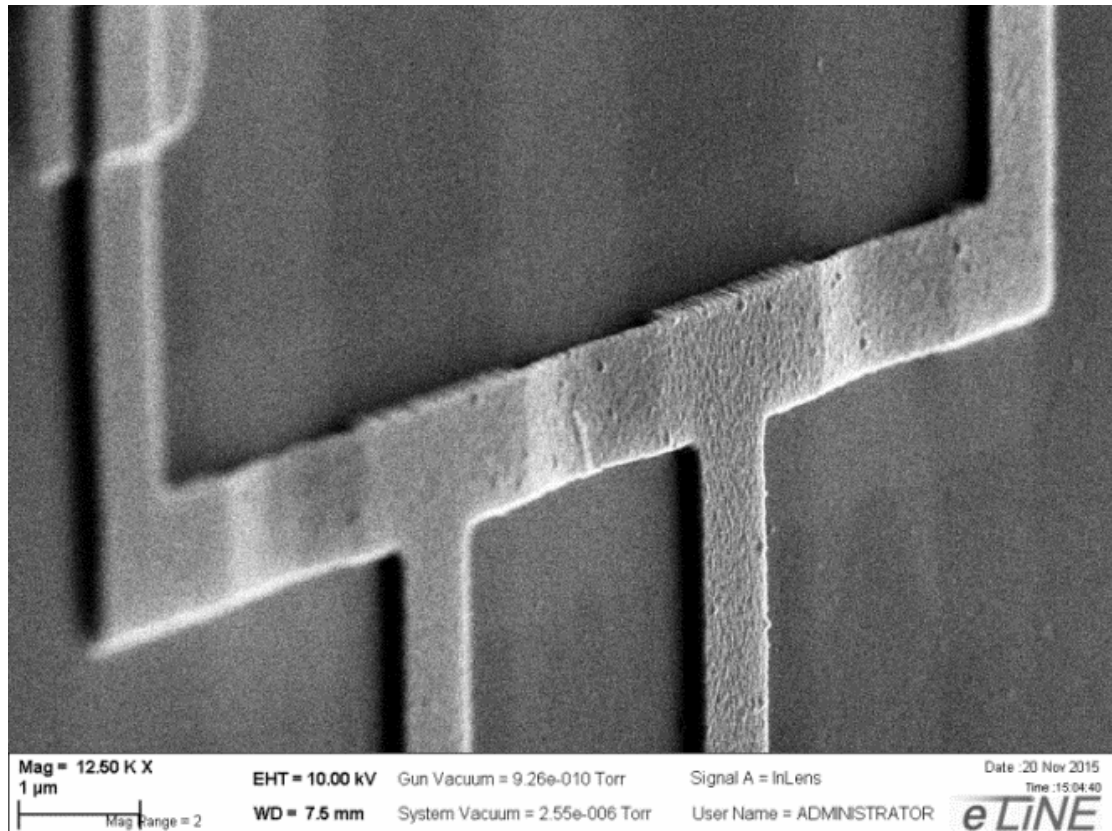


Figure 2. SEM image of fabricated sample with the test structure for dc calibration containing three suspended bridges.

sputtering, which is difficult to use for shadow evaporation. Patterning of the normal-metal- and superconducting layers can be done by the simple lift-off process. Fig. 1b shows a schematic view of the proposed layout. First, a trilayer of Ti (~10nm), Au (~50nm), and Pd (~10nm) is deposited on the substrate. This trilayer (in yellow) is patterned for wiring and contact pads followed by the deposition of the SIN structure. Superconducting Al (~100 nm) is evaporated and then oxidized in an atmosphere of pure O₂ at a pressure of 20 mbar and subsequently patterned into electrodes. Finally, the absorber normal-metal layer (20 – 30 nm of Pd or Cu) is deposited on the AlO_x on top of the Al electrodes. To form the suspended absorber bridge, we selectively etch away the Al layer under the absorber in the region defined by a window in the resist. Aluminum under the bridge region is completely removed by etching in a weak base (Microposit™ MF CD-26 developer). The results of etching are clearly visible in the scanning electron microscope (see Fig. 2).

Initially, the suspended absorbers were made of Cu. It was observed that Cu thin films are soft and have a tendency to sag down to the substrate. Besides, Cu is a good conductor at cryogenic temperatures and forms relatively low resistivity bridges even at thicknesses approaching 20 nm. This restricts the impedance matching of the device with quasioptical antennas having impedances around 50 Ω. An absorber of Cu (~20nm) with a thin (~3nm) layer of Cr was instead used to create rigid suspended bridges. While Cr+Cu is a robust thin film, care needs to be taken during subsequent fabrication steps involving resist development and liftoff. Each of these steps need to be terminated using a critical point drying step in liquid CO₂ to prevent the collapse of already-formed bridges. Rinsing in acetone, ethanol, or methanol instead of water and blow-dry with nitrogen can be alternative to critical point dryer for hard and thick Pd and Hf suspended bridges.

To investigate the influence of proximity effect on superconductivity in the S electrode of NIS junction we added in fabrication one more step of photolithography and chemical etching of Cu in

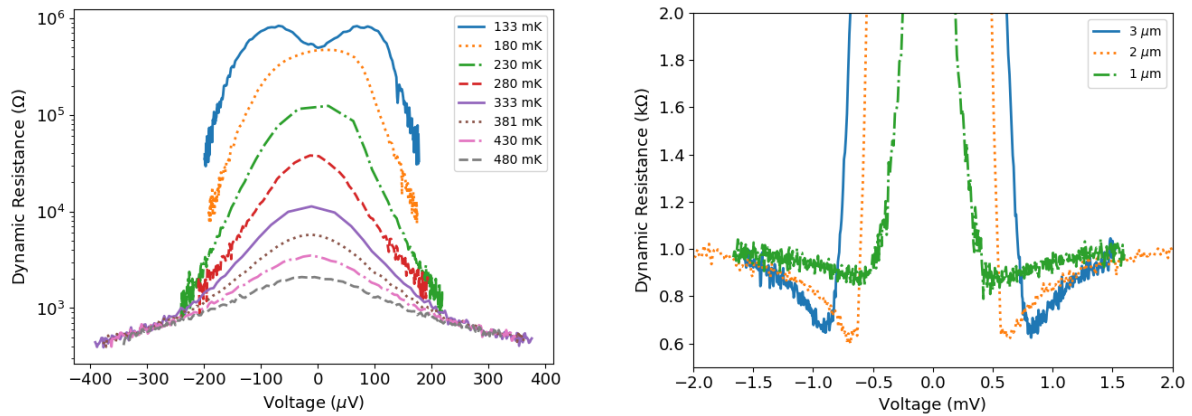


Figure 3. Dynamic resistance of the sample depicted in Fig. 1b measured in the temperature range 133–480 mK (left). Dynamic resistance of four NIS junctions connected in series with corresponding single energy gap of 0.1 mV, 0.155 mV, and 0.2 mV for samples with distance from normal-metal trap to superconducting electrode of 1, 2, and 3 μm measured at 300 mK.

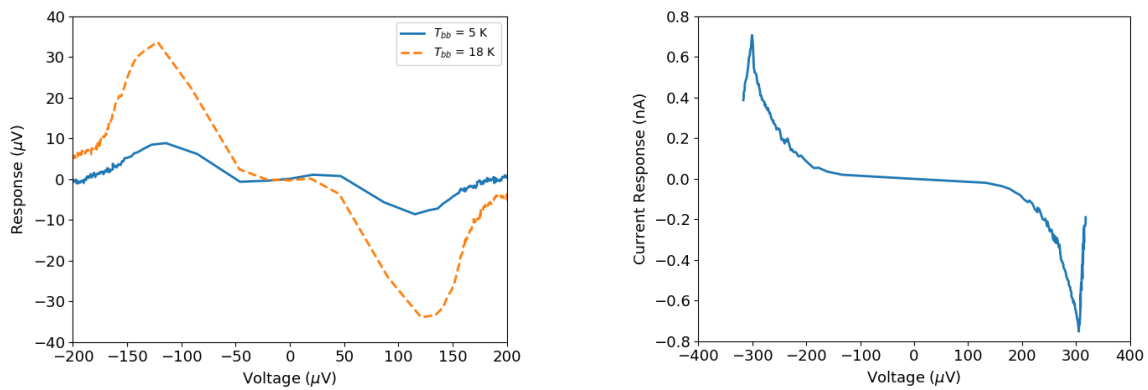


Figure 4. Voltage response of a SINIS bolometer with Hafnium suspended bridge approaching $3 \times 10^8 \text{ V/W}$ (left). The corresponding blackbody temperatures are 5 K and 18 K. Maximum current response of 0.7 nA for the suspended bolometer, corresponding to a quantum efficiency of over 15 electrons per single photon at 350 GHz (right).

diluted 1:50 HNO_3 . By this we were able to vary the distance from the golden wiring film (yellow) to the S electrode of the SIN junction (see Fig. 1c). SEM image of fabricated sample with suspended Cu bridge is presented in Fig 2. We also fabricated bolometers with Hf bridges using the above process. The higher resistivity of Hf improves the impedance matching to higher ohmic planar antennas.

3. Experimental procedure

With a 4-probe structure (Fig. 2), we were able to measure the electrical response of the bolometer by applying Joule heating across outer contacts and measuring IV curve and response for the middle contacts with single the suspended bridge. Results are presented in Fig. 3.

With Hf-based bolometers integrated in a twin-slot antenna, we measured optical response to radiation at 300 GHz. Radiation from a black body source, filtered by two band-pass filters and a neutral density filter, illuminated the sample with a twin-slot antenna which was placed on an extended hemisphere sapphire lens. Results are presented in Fig. 4 (left).

The current response can be a good indication of the quantum efficiency of the bolometer, i.e. the number of tunneling electrons n_e induced by a single photon of radiation, $\eta = n_e/n_p$. For conventional SINIS bolometers, $\eta = 1.2\text{--}1.5$ instead of the expected $\eta = hf/k_B T = 50$ at $f = 350 \text{ GHz}$, as predicted by the theory for bolometric response [3]. In the case of the suspended bolometer, with current response as in

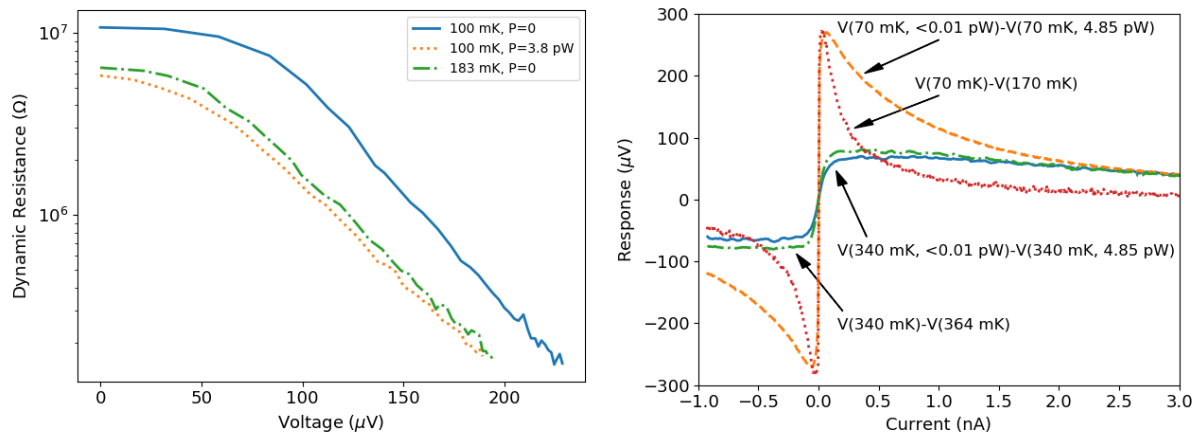


Figure 5. Dynamic resistance for phonon temperatures 100 mK and 183 mK without radiation, and for 100 mK with 3.8 pW optical power load for suspended absorber (left panel). Voltage response dependence on dc voltage for bath temperatures 70 mK and 340 mK for conventional bolometer with absorber on the substrate (right panel). Solid lines represent an estimated 4.85 pW irradiation, dashed lines represent response to equivalent increase in bath temperature without irradiation. A clear difference between thermal and optical response is visible due to non-Fermi distribution.

Fig. 4 of 0.7 nA at the incident power of 0.06 pW, the current responsivity is estimated to be $1.1 \cdot 10^4$ A/W. The current of 0.7 nA corresponds to $4.3 \cdot 10^9$ electrons per second and radiation power 0.06 pW at 350 GHz corresponds to $2.8 \cdot 10^8$ photons per second. As a result, we have a quantum gain of over 15 electrons per photon, approaching the values predicted in [3]. This is direct proof of our initial design idea to disconnect the absorber from direct contact with the substrate for improving the thermal insulation and increasing the bolometer response. Another important feature of our suspended bolometer is the similarity in the shapes of dynamic resistance to thermal and optical heating (Fig. 5, left). This shows that in such bolometers, the electron system in the absorber heated by incident radiation is thermalized, which in turn provides better quantum efficiency. In conventional bolometers with absorber on substrate we observed nonthermal optical response [4], which is a reflection of a nonequilibrium energy distribution, and is different from the expected Fermi-Dirac distribution. By means of suspending the absorber and disconnecting the phonon system from the substrate, we have managed to better thermalize hot electrons, and as a result, obtained a higher quantum gain.

4. Discussion

An important issue of SINIS bolometer and electron cooler development is proper cooling of the superconducting electrode. The simplest way is to increase the thickness and area of S electrode which helps to spread injected hot quasiparticles in a larger volume, decreasing the local hot quasiparticle density. This is critical since quasiparticle lifetimes in a superconductor like Al can be of the order of μs . Another known method is the use of a normal metal trap. One pioneering experimental works [5] shows an improvement in the cooling of a thin 18 nm Al wire with a 28 nm Cu film deposited above the Al over its oxide barrier. An improvement was observed after reducing the distance from the tunnel junction to the Cu film from 8 μm to 0.2 μm . An alternative option used a direct contact of a normal metal trap [6] where the measured trapping efficiency (the ratio of absorbed to incident power), was about 10% near 100 mK. In our earlier paper [7], normal metal traps were made of 60 nm thick Au film, with a 65 nm thick Al superconducting electrode above it. In reality, contact between Au and Al is a kind of resistive intermetallic compound with reduced transparency. This contact can be viewed as a sort of a tunnel junction with relatively high transparency, similar to [5]. In the case of Figs. 1b, and 1c, Pd is present at the top of TiAuPd trilayer, and the top Pd makes perfect contact to Al. As a result, when Pd is very close to Al, as in Fig. 1b, we have a suppression of superconductivity and no strong evidence of electron cooling. When introducing a separation of 1-2 μm as in Fig. 1c, we observe the nominal value of a double energy gap of Al ($\sim 380 \mu\text{eV}$).

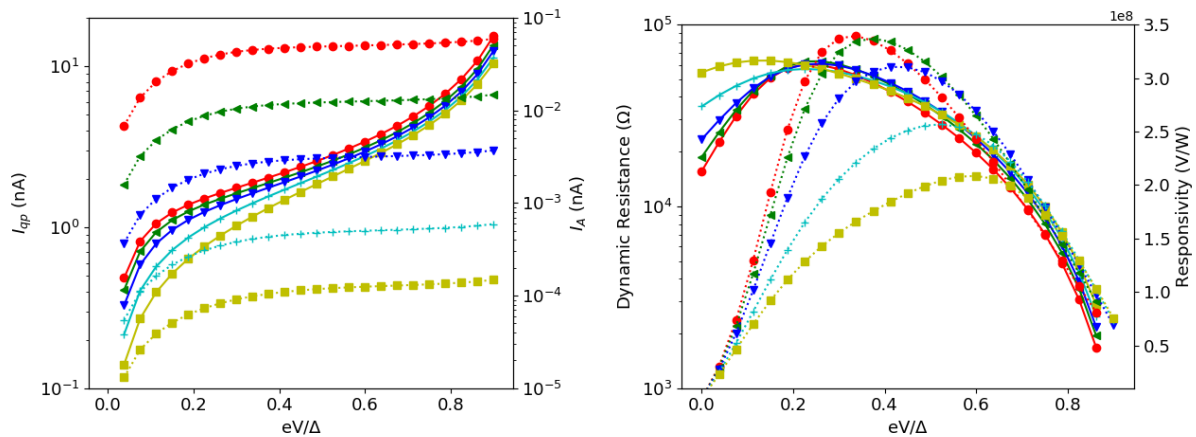


Figure 6. Relative contribution of quasiparticle (I_{qp}) and Andreev currents (I_A) to the IV characteristics of a typical SINIS bolometer with a low electron-phonon coupling absorber (left panel). Dynamic resistance and responsivity (right panel). Solid lines correspond to the left axis and dotted lines to the right axis. The various curves are simulated for normal state resistance of the NIS junction: 50 Ω (\bullet), 100 Ω (\blacktriangle), 200 Ω (\blacktriangledown), 500 Ω (+), and 1000 Ω (\blacksquare). The electron-phonon coupling constant is assumed to be 0.5 nW/ $\mu\text{m}^3\text{K}^5$, volume of the absorber 0.1 μm^3 , incident power load 0.5 pW, and a bath temperature 200 mK.

In conventional SINIS bolometer model, the presence of Andreev currents is ignored [7]. Fig. 3 (left) shows the commonly observed zero bias conductance increase which can be explained by the presence of Andreev currents with non-negligible contribution to the IV characteristics at low temperatures. Using the model developed in [8], one can predict their magnitude and study their impact on the bolometer characteristics. Fig. 6 (left) shows simulations of the relative contributions of quasiparticle and Andreev currents to the total current running in the bolometer as a function of the bias voltage normalized to the superconducting energy gap. NIS junctions with high transparency show higher contribution of Andreev currents and better electron cooling. Electron cooling increases responsivity of the device but decreases the absolute value of voltage response. Fig. 6 (right) shows a representative simulation for devices with absorbers made of materials with low electron-phonon coupling (Hf, etc). The dynamic resistance is calculated as the slope of the IV characteristics at each bias point. More details are published in [9]. A detailed study of the normal state resistance of the tunnel junctions, of Andreev currents and their impact is necessary to decide the optimum operating point of the bolometer.

Acknowledgements

This work was done with support from The Swedish Foundation for International Cooperation in Research and Higher Education (STINT, grant IG2010-14) and the Swedish Research Council (VR, grant 621-2014-5468). The clean-room processing has been done in the Nanofabrication Laboratory on the equipment sponsored by the Knut and Alice Wallenberg Foundation.

References

- [1] H. Nguyen, L. Pascal, Z. Peng, et al., Appl. Phys. Lett., v.100, 252602 (2012).
- [2] M. Tarasov, L. Kuzmin, N. Kaurova, Instr. and Experimental Techn., 52, No. 6 (2009).
- [3] I. A. Devyatov, M. Yu. Kupriyanov, JETP Letters, **80**, No. 10, 646 (2004).
- [4] M. Tarasov, V. Edelman, S. Mahashabde, L. Kuzmin, JETPh, **119**, No 1, 107 (2014).
- [5] J. Pekola, D. Anghel, T. Suppala, et al., Appl. Phys.Lett., v.76, No 19, 2782, (2000)
- [6] J. Ullom, P. Fisher, M. Nahum, Nucl. Instr.and Methods in Phys. Res., A 370, 98 (1996)
- [7] L. Kuzmin, I. Agulo, M. Fominsky, et al., Superconductor Science and Technology, 17, S400-S405 (2004)
- [8] F. J. W. Hekking, and Yu. V. Nazarov, Physical Review B, No. 49, 10 (1994).
- [9] M. Tarasov, V. Edelman, S. Mahashabde, et al., Appl. Phys.Lett., v.100, 2426, (2017)